Optical Resolution of *trans*-Bicyclo[2.2.1]heptane-2,3-diamine: Chiral Recognition in the Crystal of its Complex with (2*R*,3*R*)-*O*,*O*'-Dibenzoyltartaric Acid

Keiichiro Hatano,*[a] Tadahiro Takeda[a] and Reiko Saito[b]
[a] *Faculty of Pharmaceutical Sciences, Nagoya City University, 3-1 Tanabe-dori, Mizuho-ku, Nagoya 467, Japan*
[b] *Aichi Junior College of Nursing, Kamishidami, Moriyama-ku, Nagoya 463, Japan*

The synthesis of *trans*-bicyclo[2.2.1]heptane-2,3-diamine (**6c**), its optical resolution *via* formation of its complex with (2*R*,3*R*)-*O*,*O*'-dibenzoyltartaric acid (−BTA), and the crystal structure determination of this complex by X-ray diffraction techniques are reported. The absolute configuration of **6c** in the complex has been determined to be (*S*,*S*)-**6c** from the endowed chirality of −BTA, thus optical resolution of **6c** is achieved. Crystal data for the (*S*,*S*)-**6c**·(−BTA) complex is reported: $C_{25}H_{28}N_2O_8 \cdot 2H_2O$, $M = 520.54$, monoclinic $P2_1$, $a = 9.150(1)$, $b = 8.581(1)$, $c = 17.036(1)$ Å, $\beta = 103.30(1)°$, $V = 1301(2)$ Å^3, $Z = 2$, $R = 0.037$. The crystal of the molecular complex is found to have a multilamellar structure partitioned by thin hydrogen bonded sheets containing complex ammonium–carboxylate–water hydrogen bonds. Attached on both sides of the sheet, monolayer templates with benzoyl groups of −BTA and bicycloheptane fragments of **6c** stack with the next templates to form hydrophobic bilayers. In the monolayer template, a cavity is formed surrounded by two pairs of two benzoyl groups distinguished from each other by their orientations toward the hydrogen bond sheet. The cavity provides a final site for the chiral recognition of **6c**. The (*S*,*S*)-enantiomer of **6c** is probably distinguished from the (*R*,*R*)-enantiomer by the favourable orientation of bicycloheptane skeleton in the cavity.

One of the roots of the modern 'molecular recognition' concept comes from the classical preferential crystallization technique used in optical resolution to separate a single enantiomer from a racemic mixture. This report deals with such a model which we have encountered in the course of investigations of Pt(II) complexes with cycloalkanediamines toward potential pharmacological use as antitumour agents.[1] This case is the preparation and characterization of bicyclo[2.2.1]heptane-2,3-diamine (**6**) as a stereochemically unique ligand. This compound provides a distorted orientation of vicinal amines on the rigid and compact bicycloheptane skeleton. In addition, bicyclo[2.2.1]heptane-2,3-diamine has manifold stereochemical features: two *cis* isomers with *exo* (**6a**, equatorial with respect to the cyclohexane ring) and *endo* (**6b**, axial to it) arrangements, and *trans* (*endo*, *exo*) diastereoisomers (**6c**). We are concerned intensively with optical resolution of the *trans* diastereoisomers in conjunction with the chiral recognition model.

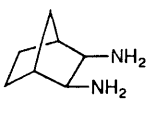

exo, exo
6a

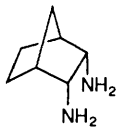

endo, endo
6b

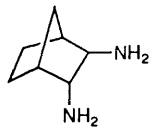

endo, exo
6c

Chiral auxiliaries of (*R*,*R*)-tartaric acid derivatives have led to the successful resolution of racemic bases through diastereoisomeric salt formation and preferential crystallization.[2] Some recent reports related to this technique are cited in ref. 3. However, the optical resolution of the **6c** diastereoisomers has never been reported. We have found that the preferential crystallization of a molecular complex salt of **6c** with (2*R*,3*R*)-*O*,*O*'-dibenzoyltartaric acid (−BTA) occurs. In order to confirm the optical resolution and the absolute configuration of the salt, X-ray crystal structure determination has been carried out. The first optical resolution for the primary vicinal diamine is reported herein, along with information about the enantioselective molecular complex formation, *i.e.*, the chiral recognition in the crystal. Since such optical resolution in the crystal is the most important origin of molecular recognition,[4] we would like to seek valuable clues as to the mechanism of the chiral recognition through detailed analysis of this crystal structure.

Experimental

General.—Melting points were measured on a Yanagimoto micromelting point apparatus and are uncorrected. The ^1H and ^{13}C NMR spectra were recorded on JEOL JNM-A500 and GSX400 spectrometers with tetramethylsilane as an internal standard. The specific optical rotation was measured using a JASCO DIP4 polarimeter. The absorption and circular dichroism (CD) spectra were recorded on a Shimadzu 210A spectrophotometer and a JASCO J600 spectropolarimeter, respectively.

Synthesis of trans-*Bicyclo*[2.2.1]*heptane*-2,3-*diamine* **6c**.—The synthetic route to **6c** employed in the present study is shown in Scheme 1. Bicyclo[2.2.1]hept-5-ene-2,3-dicarboxylic anhydride (**1**, 250 g; Tokyo Kasei Co. Ltd) was converted to its dimethyl ester (**2**, yield 176 g, 55%) by a method similar to that reported in the literature.[5] Compound **2** was epimerized by the method of Meinwald and Gassman[6] with slight modification. A mixture of **2** and CH_3ONa (28%) in methanol (*ca.* 2 dm^3) was refluxed for 3 days (**2**→**3**). The reaction mixture was added to water for hydrolysis (**3**→**4**), refluxed again for 1.5 h, and then reduced to dryness. To the resulting solid, conc. HCl (250 cm^3) was added. The solid residue was filtered, washed with water and then recrystallized twice from ethanol–water (1:2) to give **4** (yield 120 g, 79%). The hydrogenation of **4** (24 g), catalysed by Rh–Pd/C, afforded **5** quantitatively. A total 250 g of **5**, collected

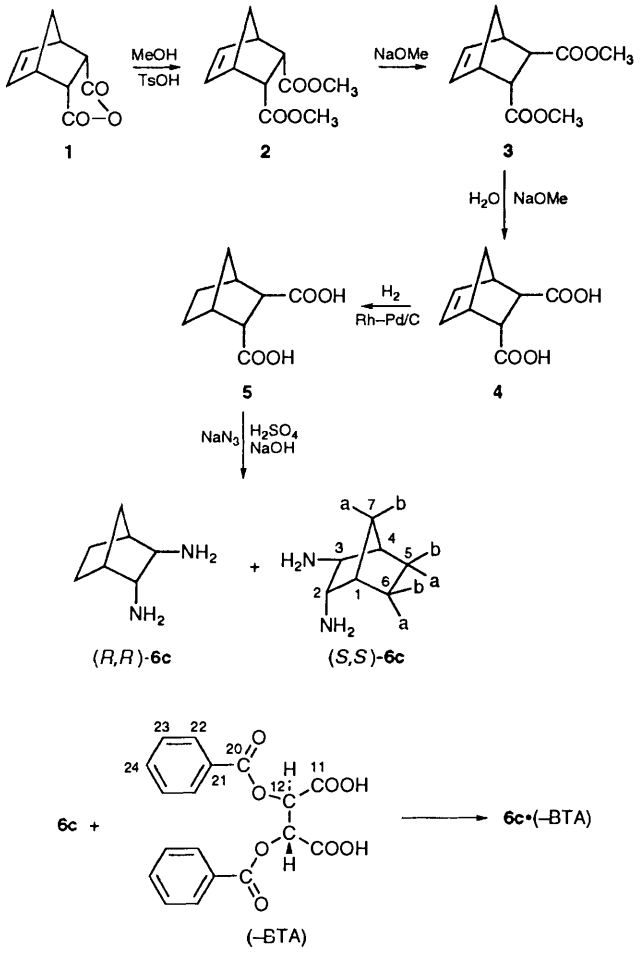

Scheme 1

Table 1 Summary of crystal data and intensity collection parameters for the complex **6c**•(−BTA)

Formula	$C_{25}H_{28}N_2O_8$•$2H_2O$
M	520.54
Crystal dimensions/mm^3	0.36 × 0.75 × 0.12
Space group	$P2_1$
T/K	293
a/Å	9.150(1)
b/Å	8.581(1)
c/Å	17.036(1)
β/°	103.30(1)
V/Å^3	1301(2)
Z	2
Calcd. density D_c/ g cm^{-3}	1.328
Obsd. density D_m/g cm^{-3}	1.323
Radiation	Graphite monochromated Mo-Kα
2θ Range	3–50°
Scan technique	ω–2θ
Scan range (ω/°)	0.65 + 0.35 tanθ
No. of measured data	2530
Criterion for observation	$F_o > 3\sigma(F_o)$
Unique obsd. data	2251
R	0.037
R_w[a]	0.036
No. of variables	334

[a] $R_w = \{[\Sigma w(|F_o| - |F_c|)^2]/[\Sigma w(F_o)^2]\}^{\frac{1}{2}}$ where $w = 1$.

through such syntheses, was subjected to amination by Schmidt's method[7] to yield HCl salts of **6** (140 g, 52%). Free diamine liberated by KOH treatment of **6**–HCl (140 g) was distilled under reduced pressure (8 mmHg) to give 40 g of distillate at 135–145 °C (45% yield). Preliminary NMR study suggested that only *trans* isomer **6c** was present in the distillate.

Optical Resolution of **6c**.—The **6c** racemate (3.0 g) in water (10 cm^3) was mixed with −BTA (6.3 g) in propan-2-ol (15 cm^3). The white precipitate was separated by filtration, washed with water and recrystallised twice from *N*,*N*-dimethylformamide (DMF)–H_2O (1:2) to give the **6c**•(−BTA) (1:1) complex (1.9 g, 16% yield based on racemate). In the ^{1}H NMR data below, the starred multiplicities are intrinsically multiplets, but the main feature of the spin–spin couplings, omitting those lower than 2 Hz, is given. M.p. 176–177 °C (decomp.) (Found: C, 57.7; H, 6.1; N, 5.35. $C_{25}H_{28}N_2O_8$•$2H_2O$ requires C, 57.69; H, 6.20; N, 5.38%); $[\alpha]_D^{20}$ −83.4 (*c* 1.0, MeOH); δ_H(400 MHz; CD_3OD) 1.34–1.39 (1 H, m, 5a-H), 1.45 (1 H, d*, J_{gem} 11, 7b-H), 1.49–1.58 (2 H, m, 6a-, 6b-H), 1.67–1.74 (1 H, m, 5b-H), 1.80 (1 H, d*, J_{gem} 11, 7a-H), 2.34 (1 H, d*, J_{5b-H} 4.3, 4-H), 2.50 (1 H, s*, 1-H), 3.00 (1 H, s*, 3-H), 3.41 (1 H, s*, 2-H), 5.79 (2 H, s, 12-, 13-H), 7.45–7.48 (4 H, m, *m*-Ph), 7.57–7.60 (2 H, m, *p*-Ph) and 8.13–8.15 (4 H, m, *o*-Ph); δ_C 20.97 (C-6), 27.72 (C-5), 35.75 (C-7), 41.45 (C-1), 42.69 (C-4), 58.96 (C-3), 59.13 (C-2), 76.89 (C-12, -13), 129.45 (C-23, -25, -33, -35), 131.07 (C-22, -26, -32, -36), 131.69 (C-21, -31), 134.23 (C-24, -34), 167.90 (C-20, -30) and 174.01 (C-11, -14).

Treatment of **6c**•(−BTA) with HCl (3 mol dm^{-3}) afforded the HCl salt of (+)-**6c** (Found: C, 42.2; H, 8.2; N, 14.0. $C_7H_{14}N_2$•2HCl requires C, 42.23; H, 8.10; N, 14.00%); $[\alpha]_D^{20}$ +26.0 (*c* 2.0, CH_3OH); δ_H(400 MHz; CD_3OD) 1.45–1.51 (1 H, m, 5a-H), 1.53–1.56 (1 H, m, 6a-H), 1.58 (1 H, d*, J_{gem} 11, 7b-H), 1.64–1.70 (1 H, m, 6b-H), 1.79–1.86 (1 H, m, 5b-H), 1.90 (1 H, d*, J_{gem} 11, 7a-H), 2.47 (1 H, d*, J_{3-H} 4.0, 4-H), 2.67 (1 H, s*, 1-H), 3.13–3.15 (1 H, m, 3-H) and 3.54–3.56 (1 H, m, 2-H); δ_C 20.84 (C-6), 27.47 (C-5), 35.62 (C-7), 41.01 (C-1), 42.12 (C-4), 58.39 (C-3) and 58.70 (C-2).

Crystal Structure Determination and Refinement.—A transparent crystal of **6c**•(−BTA), in the form of plate, was examined on an Enraf–Nonius CAD4 Kappa goniometer using Mo-Kα radiation. The preliminary examination established a monoclinic unit cell containing two complexes. A least-squares refinement of the setting angles of 25 reflections, collected in the range of 18° < 2θ < 24°, led to the cell constants. Details of the intensity collection and crystal data are summarized in Table 1. Intensity data were corrected for Lorentz and polarization effects but not for absorption (μ = 0.97 cm^{-1}).

The structure was solved by the direct method and refined by full-matrix least-squares techniques. The systematic absence of the reflections indicated the non-centrosymmetric space group $P2_1$ and the subsequent developments of the structure analysis proved it to be the correct choice. The most non-hydrogen atoms were located in an initial E-map. After few cycles of refinements and difference Fourier syntheses, a molecular model consistent with the chemical structure was found. Hydrogen atoms bound to ammonium nitrogen and water oxygen were found in a difference Fourier map. These hydrogens were refined partially and regularized, and then used as fixed parameters. Other hydrogens bound to carbon were included in calculated positions as fixed parameters. At this stage of refinement, the enantiomorph was adjusted on the basis of the known configuration of −BTA. The final model utilizing anisotropic thermal parameters for all non-hydrogen atoms and fixed hydrogen atoms parameters were carried to convergence by the repeated least-squares refinements. The final difference Fourier was judged to be essentially featureless; the largest peak had a height of 0.17 e Å^{-3} and was located near C-32. Tables of final positional and thermal parameters, and lists of bond distances and angles have been deposited at the

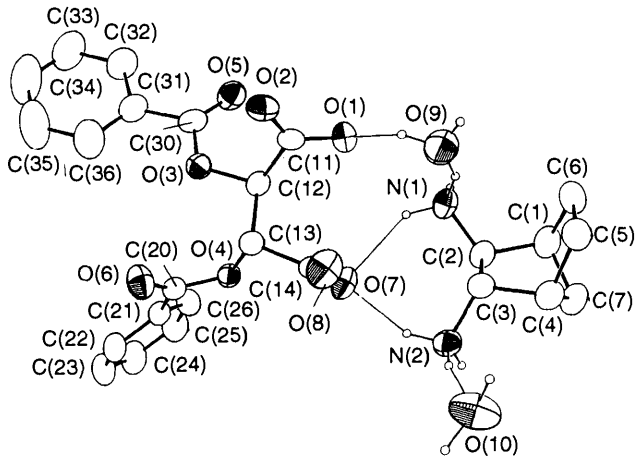

Fig. 1 Perspective view of the X-ray structure of **6c**·(−BTA) with atomic labelling. Octant-shaded ellipsoids are heteroatoms and all thermal ellipsoids are contoured at the 50% probability level. Some hydrogens involved in hydrogen bond system are shown as arbitrary circles.

Cambridge Crystallographic Data Centre.* Programs and computers used and sources of scattering factor data are given in ref. 21.

Results and Discussion

Synthesis and NMR Spectra.—The compounds **6c** and **6a** (perhaps **6b**, too) have been prepared previously, through reduction of dinitro-[8] or 2-nitroxime-3-nitro-bicyclo[2.2.1]-heptane[9] or the cobalt complex of the analogous compound[10] by other workers. However, since those investigations did not target the preparation of bicyclo[2.2.1]heptane-2,3-diamines, the isolation and NMR spectral characterization of each isomer seemed not yet complete. In the present work, the synthetic route to **6c** in Scheme 1 was chosen because of readily available starting materials, expected high yield, and probable by-production of **6a** and/or **b**. We attempted to prepare **6b** or **a** through the plausible direct conversion of *cis*-bicyclo[2.2.1]-heptane-2,3-dicarboxylic acid, which may be derived by shortening or elongating the epimerization reaction from **2** to **3**, but failed to detect any trace of **6b** or **a** in the final product. The exclusive formation of **6c** is probably due to the steric repulsion between vicinal substituents, although the details of the stereochemical reaction mechanism for the present synthetic route is as yet unknown.

The proton NMR measurements of **6c**–HCl in D_2O have been reported[9] but the assignments were incomplete and misleading. The ^{13}C NMR chemical shifts in many bicycloheptyl derivatives have been reported,[11] but those of **6c** have not been included. We made complete assignments of ^1H and ^{13}C resonances of **6c**–HCl based on cross correlations in the ^{13}C–^1H and ^1H–^1H COSY (correlated spectroscopy), and ^1H–^1H NOESY† (nuclear Overhauser and exchange spectroscopy) maps, and the results are reported in the Experimental section. None of the carbon nor proton resonances of the bicycloheptane fragment are equivalent, suggesting an anisotropic magnetic environment in **6c**. The ^1H and ^{13}C NMR resonances of the **6c**·(−BTA) complex in CD_3OD have been assigned on the basis of those of **6c**–HCl and −BTA. Because of symmetry, there are half as many resonances as atoms in the NMR spectra of the −BTA moiety. All of the ^1H resonances of the bicycloheptane fragment of the complex shift upfield by δ 0.11–0.16 from those of **6c**–HCl. The upfield shifts can be ascribed to the ring current effects[12] of the phenyl groups of −BTA.

Molecular Structure and Stereochemistry of **6c**·(−BTA).—The molecular structure of **6c**·(−BTA) determined in this work is shown in Fig. 1. On the basis of the known (*R*,*R*) configuration of −BTA, the absolute configuration of **6c** in the crystal could be determined to be (*S*,*S*)-**6c** by this model. The optical rotation measurement of dextrorotary **6c** isolated from the crystal has confirmed that optical resolution of (*S*,*S*)-**6c** is achieved through the preferential crystallization of this complex.

The present structure analysis includes the simultaneous determination of the geometries of two molecular ions: *trans*-bicyclo[2.2.1]heptane-2,3-diammonium ion and *O*,*O*′-dibenzoyltartarate anion. Some interesting points about the geometry of individual molecular ions will be discussed below.

As to the molecular geometry of the bicycloheptane fragment, there are many reports on X-ray structures of various bicycloheptane derivatives,[13,15b] and a statistical review[14a] of the bond parameters of this fragment found in the period 1976–1980, combined with gas-phase electron diffraction data,[14b] is also available. However, a simple derivative such as **6c** is still one of few X-ray instances, owing to difficulties of obtaining suitable single crystals. In addition, the free bicycloheptane skeleton has been examined recently as a control to estimate a new force field in molecular mechanic calculations.[15a] It may be intriguing to compare present bond parameters with those from the calculations or the statistical data.[14] The comparison is summarized in Table 2. These parameters are generally in good agreement with the calculations[15a] and the statistics,[14] within double of the experimental errors despite that there could be influence due to the vicinal diamine substituents. The tendency of the C(2)–C(3) bond to be slightly longer than the other bonds has been pointed out as one of the reasons why the force field needs renewal.[15a] The elongation of the C(2)–C(3) type has been ascribed to the eclipsed conformation about the bond. However, it is difficult to draw a correlation between the very small differences in bond lengths and the bond angles and/or torsion angles. The observed large differences in the torsion angles are remarkable; the maximum one is 11.8° found between C(6)–C(1)–C(2)–C(3) and C(5)–C(4)–C(3)–C(2). The deviations reflect, we think, the flexibility or deformity of the apparently symmetrical bicycloheptane skeleton. Such angular deformity was found previously in relatively rigid ring systems, *e.g.*, the diazepino–oxazole ring system,[16] and may be a cause of the conformational asymmetry. However, the conformational asymmetry, as demonstrated first by Gilman *et al.*[17] for 1,4-benzodiazepine derivatives, is unlikely to exist in the present bicycloheptane system because of its skeletal non-convertibility. Torsion angles involving amines are shown schematically as the Newman projection of the C(2)–C(3) bond in Fig. 2 in comparison with those of the tartaric acid moiety.

To our knowledge, there is only one published crystral structure including the dibenzoyltartaric acid moiety: *O*,*O*′-dibenzoyl-*N*,*N*,*N*′,*N*′-tetramethyltartramide (BTAA).[18] The important stereochemistry of this kind of molecule must be its conformation. Fig. 2 shows the Newman projection of the C(12)–C(13) bond with some torsion angles concerned. The *gauche* conformation of carboxylic acid groups (*anti* arrangement of hydrogens) is the same as that of BTAA in the crystal, although the *anti* conformation (hydrogens *gauche*) was speculated[18] for −BTA in methanol from the CD spectrum. The CD spectrum of **6c**·(−BTA) in methanol is the same as

* For details of the CCDC deposition scheme, see 'Instructions for Authors', *J. Chem. Soc., Perkin Trans. 2*, 1994, issue 1.

† The ^1H–^1H NOESY spectrum of **6c**–HCl has been deposited under the Supplementary Publications Scheme. For details of the scheme, see 'Instructions for Authors', *J. Chem. Soc., Perkin Trans. 2*, 1994, issue 1 [Suppl. Publ. No. 56988 (3 pp.)].

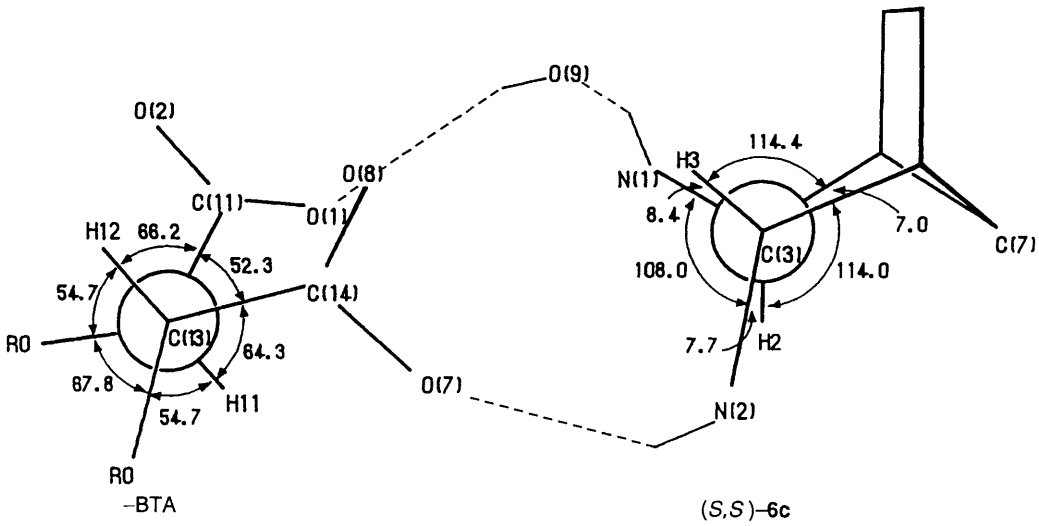

Fig. 2 Newman projections along the C(2)–C(3) and C(12)–C(13) bonds for (*S,S*)-**6c** and −BTA, respectively. The two bonds are not parallel in the real complex salt.

Table 2 Comparison of structural parameters of the bicycloheptane fragment

	X-Ray (mean)[a,14a]	MM3[15a]	This work[a]
Bond lengths (Å)			
C(1)–C(2)	1.546(23)	1.548	1.535(8)
C(2)–C(3)	1.559(19)	1.557	1.546(8)
C(1)–C(7)	1.539(22)	1.540	1.538(2)
$\langle CC \rangle_{av}$	1.548(8)	1.548	1.538(8)
Bond angles (°)			
C(1)–C(2)–C(3)	102.6(16)	103.3	103.4(3)
C(2)–C(1)–C(6)	107.1(46)	107.9	108.6(21)
C(2)–C(1)–C(7)	101.7(25)	101.3	101.1(17)
C(1)–C(7)–C(4)	94.2(11)	95.0	94.5(4)
Torsion angles (°)			
C(6)–C(1)–C(2)–C(3)	71.6	71.0	70.5(48)
C(2)–C(1)–C(7)–C(4)	55.5	55.5	55.8(18)
C(7)–C(1)–C(2)–C(3)	35.1	34.9	35.3(47)
C(1)–C(2)–C(3)–C(4)	4.8	0.0	4.2(39)

[a] The standard deviations of the least significant digits are given in parentheses.

that of −BTA alone, affording no useful information about the conformation in solution. The VCD (vibrational circular dichroism) spectrum[19] of −BTA is not available. The NMR resonance of ^{13}C satellites[20] of 12-H and 13-H could not be resolved well for $^3J_{HH}$ of the ABX system in the present work. Hence the conformation of −BTA in the solution state is as yet unknown. The conformation established in the solid state is assumed, in general, to be retained in solution as the most stable form in the spectroscopic studies.[18,20,21]

Hydrogen Bonds and Crystal Packing.—Part of the hydrogen bonding between the molecular complex and two water molecules is shown in Fig. 1. Since the whole hydrogen bonding system in the crystal is somewhat complex to describe, some important short atomic distances are reported here: O(1)–O(9), 2.775; O(2)–N(1′), 2.700; O(7)–O(10′), 2.701; O(8)–N(2′), 2.773; N(1)–O(9), 2.858; N(1)–O(1), 2.901; N(2)–O(10), 2.846; N(2)–O(7), 2.884 Å. The hydrogen bond system includes two different atomic interaction modules, *e.g.*, the two water molecules play different roles in the interactions. Notably, there is a O(9)–O(5′) (2.905 Å) interaction, whereas the other benzoyl oxygen, O(6), is isolated from water and contained in a hydrophobic space. Thus, the two benzoyl groups of −BTA orientate themselves differently from one another with respect to the hydrogen bond system. Consequently, the hydrogen bond system provides two recognition sites, distinguished by the benzoyl orientations, which must be involved in the three-site module needed for the general chiral recognition process.

Before discussing the individual enantiomers of **6c**, we should inspect the crystal packing to locate the crucial factor for chiral recognition, *i.e.*, the third site of the module. The hydrogen bond system develops two-dimensionally in the crystal, making a sheet of hydrogen bond nets with *ca.* 2 Å thickness parallel to the *ab* plane, as shown in Fig. 3. The diagram is a view of a cross section of the molecular stacking and shows a multi-lamellar structure. Each layer is composed of a hydrogen bond sheet and a hydrophobic bilayer of *ca.* 15 Å thickness. From another viewpoint, a unit layer can be assigned to the central hydrogen bond sheet, sandwiched by two rugged hydrophobic templates, just like a wafer cake. Top and bottom templates of this unit layer have an identical chirality and are ready to make an asymmetric bilayer with the next unit. In other words, in the arrangement of a bicycloheptane fragment and two non-equivalent benzoyl fragments in a template, triangular bases formed by the three fragments can be disposed in a chiral mode as shown schematically in Fig. 4. Such a chiral disposition is a general feature of the assembly of molecules containing a chiral moiety. An important point is that the chirality of **6c** is independent of the asymmetry of the chiral layered structure, *i.e.*, whichever enantiomer, (*S,S*)-**6c** or (*R,R*)-**6c**, was accommodated into the unit layer, the chiral bilayer would still be conserved. Consider also that the same chiral layered system must be adopted for the (*R,R*)-**6c**·(+BTA) [+BTA = (2*S*,3*S*)-*O*,*O*′-dibenzoyltartaric acid] crystal as the mirror image.

Thus, the preference for complexation with (*S,S*)- or (*R,R*)-**6c** should not be attributed to the layered structure in this case, although Gould *et al.*[4] suggested some differences in efficacy between monolayer and bilayer when brucine and strychnine crystallize preferentially with D and L enantiomers of *N*-benzoylalanine, respectively. The preference must depend on the shape of the cavity, as has also been pointed out by them,[4] but ambiguously as the chiral cavity. A cavity for (*S,S*)-**6c** formed in the template is not necessarily chiral in shape but must offer the final site of the chiral recognition module. In this context, the driving force exerted to select (*S,S*)-**6c** seems to exist in the crystallization process where some host molecules begin to assemble into a small wafer unit with hydrogen bond formation. The assembly will simultaneously determine the shape of the cavity so as to accommodate the preferred chiral guests.

Chiral Molecular Recognition.—The key questions concerning chiral recognition of this molecular complex are why the −BTA host does not select (*R*,*R*)-**6c** as the partner and what the shape of the cavity is. Unfortunately, since the crystals of the −BTA complex with (*R*,*R*)-**6c** or racemic **6c** (no resolution) could not be obtained so far, the direct characterization or comparison of the cavity for (*R*,*R*)-**6c** with that for (*S*,*S*)-**6c** is not possible. We have examined instead what happens if (*S*,*S*)-**6c** is substituted by (*R*,*R*)-**6c** in the real cavity of −BTA, using molecular graphical models.*

The cavity for the bicycloheptane fragment has been found to be a simple box placed on the hydrogen bonded sheet, four benzoyl moieties surrounding it as side walls and another benzoyl group from the next layer acting as an opened top lid (see Figs. 3 and 4). The substitution should be operated in the box by fixing two nitrogen positions, so as to keep the two recognition sites intact on the hydrogen bond system, and by setting the centre of **6c** shifted as little as possible in the cavity. This operation could be performed with the shifts of the three positions as small as 0.02 Å in the models. Fig. 5 shows a schematic diagram of the model of the cavity arrangement and the possible orientations of **6c** racemates, (*S*,*S*)-**6c** and (*R*,*R*)-**6c**.

* A FORTRAN program was written using the ORTEP II algorithms for this specific model study.

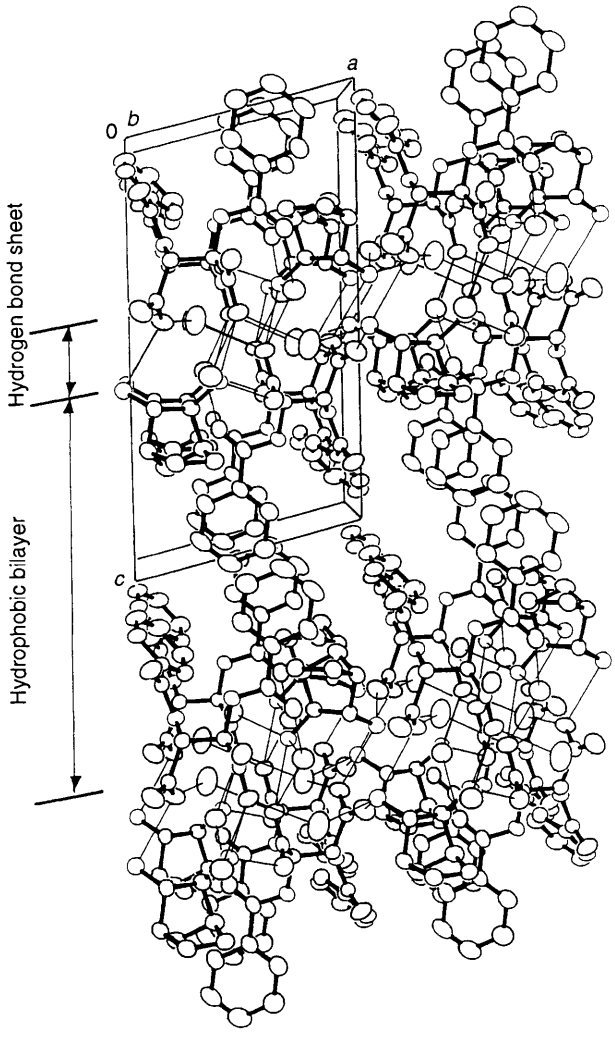

Fig. 3 The unit cell and the lattice arrangement of the **6c**·(−BTA) complex as projected on the *ac* plane. The atomic interactions of 2.7–3.0 Å involved in the hydrogen bonds are indicated by thin lines. All hydrogens and one water oxygen [O(10)] are omitted for clarity.

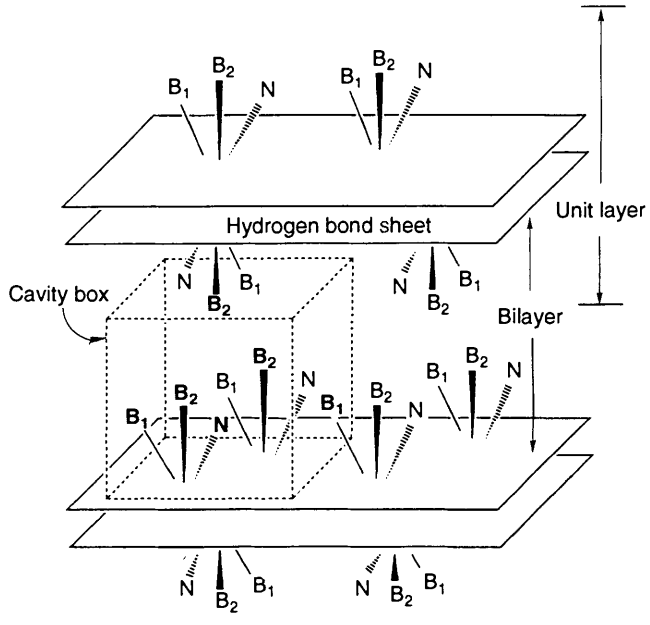

Fig. 4 Schematic representation of the chiral layered arrangement. B_1 and B_2 symbolise two benzoyl groups of −BTA standing on the hydrogen bond sheet, respectively. N denotes the bicycloheptane fragment of **6c**. Boldface symbols show those groups involved in the cavity box.

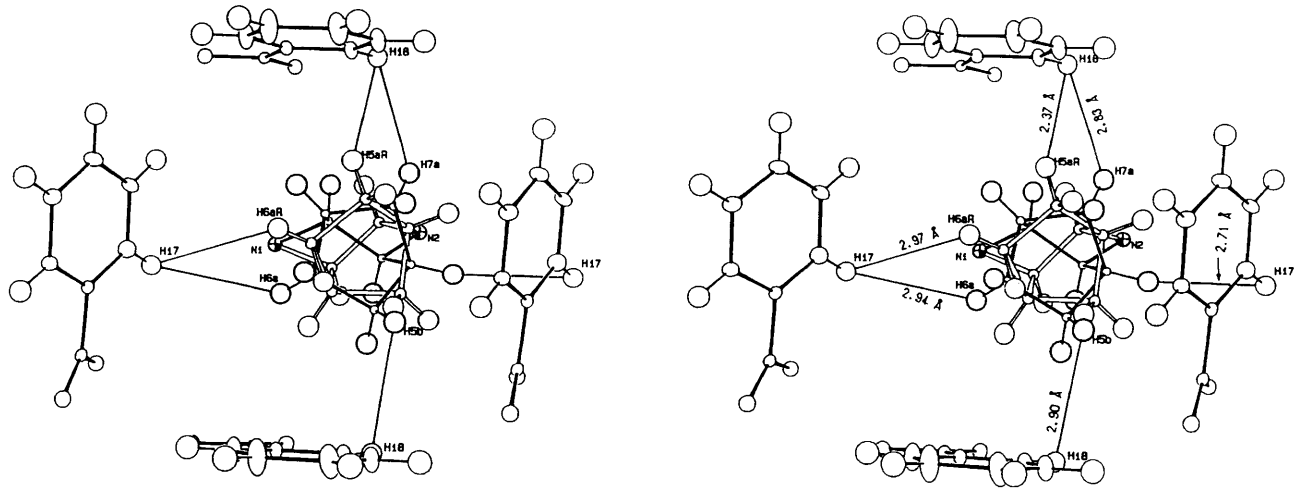

Fig. 5 Schematic stereoview of the bicycloheptane fragment orientations in the cavity. The heavy and open bonds are demonstrated for orientations of (*S*,*S*)-**6c** and (*R*,*R*)-**6c**, respectively. Some H · · · H interactions are shown with the atomic distances.

This model of the substrate–cavity contacts is just like inserting a pentagonal **6c** wrapped by hydrogen atoms into a square box of the cavity. In the cavity, the real orientation of (*S*,*S*)-**6c** has some H ••• H atomic interaction, with distances in the range of 2.70 to 3.00 Å which are essentially of the van der Waals type. On the other hand, hydrogen atoms of (*R*,*R*)-**6c** also interact normally with benzoyl atoms, except for one close H ••• H interaction, 5_{aR}-H ••• 18-H (2.37 Å), as shown in Fig. 5. Such a 'near miss' of H ••• H for (*R*, *R*)-**6c** is unavoidable inasmuch as the two nitrogen positions and the rigidity of the bicycloheptane skeleton are maintained, with only small rotation about the N(1)–N(2) vector allowed in the cavity. For quantitative evaluation of the optimum orientation of (*R*,*R*)-**6c** and the free energy difference, all the interatomic interactions involved in the cavity should be considered; however, this was impossible since accurate and reliable potential functions were not available.* From the qualitative viewpoint, the spatial atomic distance of *ca.* 2.4 Å for H ••• H must be repulsive or, at least, far from the potential minimum of the intermolecular interatomic force that is of attractive nature. Therefore, the emergence of such repulsions by the insertion of (*R*,*R*)-**6c** into the real cavity of (*S*,*S*)-**6c** must be an essential factor to exclude the (*R*,*R*)-enantiomer from the crystal formation. It is concluded in this model study that the chiral recognition of (*S*,*S*)-**6c** in the preferential crystallization of the complex with −BTA has been achieved through the exclusion of (*R*,*R*)-**6c** from the cavity of −BTA owing to the unfavourable orientation.

* In the radial distribution curve for the gas-phase molecule,[15] relatively large deviation has been observed in the range 2.7–3.5 Å. It is doubtful that the same functions apply to the intermolecular atomic interactions.

References

1 (*a*) M. Goto, J. Hirose, M. Noji, K.-I. Lee, R. Saito and Y. Kidani, *Chem. Pharm. Bull.*, 1992, **40**, 1022; (*b*) R. Saito and Y. Kidani, *Bull. Chem. Soc. Jpn.*, 1984, **57**, 3430.

2 J. Jaques, A. Collet and S. H. Wilen, *Enantiomers, Racemates and Resolutions*, Wiley–Interscience, New York, 1981.

3 (*a*) Y. Dobashi, S. Hara and Y. Iitaka, *J. Org. Chem.*, 1988, **53**, 3894; (*b*) F. Toda and K. Tanaka, *J. Org. Chem.*, 1988, **53**, 3607; (*c*) P. Mangeney, F. Grojean, A. Alexakis and J. F. Normant, *Tetrahedron Lett.*, 1988, **29**, 2675.

4 R. O. Gould and M. D. Walkinshaw, *J. Am. Chem. Soc.*, 1984, **106**, 7840.

5 C. C. Arthur and C. H. Elbert, in *Org. Synth.*, 1963, Coll. Vol. IV, p. 304.

6 J. Meinwald and P. G. Gassman, *J. Am. Chem. Soc.*, 1960, **82**, 5445.

7 N. W. Werner and J. Casanova, Jr., *Org. Synth.*, 1973, Coll. Vol. V, p. 273.

8 H. Shechter, J. J. Gardikes, T. S. Cantrell and G. V. D. Tiers, *J. Am. Chem. Soc.*, 1967, **89**, 3005.

9 M. Scheinbaum, *J. Org. Chem.*, 1968, **33**, 2586.

10 P. N. Becker, M. A. White and R. G. Bergman, *J. Am. Chem. Soc.*, 1980, **102**, 5676.

11 J. B. Grutzner, M. Jautelat, J. B. Dence, R. A. Smith and J. D. Roberts, *J. Am. Chem. Soc.*, 1970, **92**, 7107.

12 C. E. Johnson and F. A. Bovey, *J. Chem. Phys.*, 1958, **29**, 1012.

13 Recent X-ray structures including the bicycloheptane fragments: (*a*) C. Eaborn and P. B. Hichcock, *J. Chem. Soc., Perkin Trans. 2*, 1991, 1137; (*b*) Y. Yang, F. Diederich and J. S. Valentine, *J. Am. Chem. Soc.*, 1991, **113**, 7179; (*c*) L. A Paquette, D. T. DeRussy, T. Vandenheste and R. D. Rogers, *J. Am. Chem. Soc.*, 1990, **112**, 5562; (*d*) K. Tatsumi, I. Matsubara, Y. Inoue, A. Nakamura, K. Miki and N. Kasai, *J. Am. Chem. Soc.*, 1989, **111**, 7766.

14 (*a*) L. Doms, D. Van Hemelrijk, W. Van de Mieroop, A. T. Lenstra and H. J. Geise, *Acta Crystallogr., Sect. B, Struct. Sci.*, 1985, **41**, 270; (*b*) L. Doms, L. Van den Enden, H. J. Geise and C. Van Alsenoy, *J. Am. Chem. Soc.*, 1983, **105**, 158.

15 (*a*) N. L. Allinger, H. J. Geise, W. Pyckhout, L. A. Paquette and J. C. Gallucci, *J. Am. Chem. Soc.*, 1989, **110**, 1106; (*b*) M. G. Newton, N. S. Pantaleo, S. Kirbawy and N. L. Allinger, *J. Am. Chem. Soc.*, 1978, **100**, 2176.

16 K. Hatano, Y. Kurono, T. Kuwayama, A. Murakami, T. Yashiro and K. Ikeda, *J. Pharm. Sci.*, 1991, **80**, 1096.

17 N. W. Gilman, P. Rosen, J. V. Earley, C. Cook and L. J. Todaro, *J. Am. Chem. Soc.*, 1990, **112**, 3969.

18 J. Gawronski, K. Gawronska and U. Rychlewska, *Tetrahedron Lett.*, 1989, **30**, 6071.

19 P. L. Polavarapu, C. S. Ewig and T. Chandramouly, *J. Am. Chem. Soc.*, 1987, **109**, 7382.

20 J. Ascenso and V. M. S. Gil, *Can. J. Chem.*, 1980, **58**, 1376.

21 K. Hatano, Y. Kurono, T. Kuwayama, H. Tamaki, T. Yashiro and K. Ikeda, *J. Chem. Soc., Perkin Trans. 2*, 1992, 621.

Paper 3/04597H
Received 2*nd August* 1993
Accepted 18*th October* 1993